Published for SISSA by Springer

Received: March 9, 2021
Accepted: April 21, 2021
Published: May 12, 2021

Observation of the decay $\Lambda_b^0 \to \chi_{c1} p \pi^-$

The LHCb collaboration

E-mail: Ivan.Belyaev@itep.ru

Abstract: The Cabibbo-suppressed decay $\Lambda_b^0 \to \chi_{c1} p \pi^-$ is observed for the first time using data from proton-proton collisions corresponding to an integrated luminosity of $6\,\text{fb}^{-1}$, collected with the LHCb detector at a centre-of-mass energy of 13 TeV. Evidence for the $\Lambda_b^0 \to \chi_{c2} p \pi^-$ decay is also found. Using the $\Lambda_b^0 \to \chi_{c1} p K^-$ decay as normalisation channel, the ratios of branching fractions are measured to be

$$\begin{aligned}
\frac{\mathcal{B}(\Lambda_b^0 \to \chi_{c1} p \pi^-)}{\mathcal{B}(\Lambda_b^0 \to \chi_{c1} p K^-)} &= (6.59 \pm 1.01 \pm 0.22) \times 10^{-2}\,, \\
\frac{\mathcal{B}(\Lambda_b^0 \to \chi_{c2} p \pi^-)}{\mathcal{B}(\Lambda_b^0 \to \chi_{c1} p \pi^-)} &= 0.95 \pm 0.30 \pm 0.04 \pm 0.04\,, \\
\frac{\mathcal{B}(\Lambda_b^0 \to \chi_{c2} p K^-)}{\mathcal{B}(\Lambda_b^0 \to \chi_{c1} p K^-)} &= 1.06 \pm 0.05 \pm 0.04 \pm 0.04\,,
\end{aligned}$$

where the first uncertainty is statistical, the second is systematic and the third is due to the uncertainties in the branching fractions of $\chi_{c1,2} \to J/\psi\gamma$ decays.

Keywords: B physics, Branching fraction, Hadron-Hadron scattering (experiments), QCD, Quarkonium

ArXiv ePrint: 2103.04949

https://doi.org/10.1007/JHEP05(2021)095

JHEP05(2021)095

Contents

1 Introduction

The amplitude analyses of the beauty-baryon decays $\Lambda_b^0 \to J/\psi p K^-$ established the existence of a new class of baryonic resonances in the $J/\psi p$ system, hidden-charm pentaquarks, that cannot be described within the simplest pattern of baryon structure consisting of three constituent quarks [1–3]. Evidence for a pentaquark contribution in the same $J/\psi p$ mass region was obtained in the study of the Cabibbo-suppressed decays $\Lambda_b^0 \to J/\psi p \pi^-$ [4]. Recently, further evidence for a new pentaquark candidate in the $\Xi_b^- \to J/\psi \Lambda K^-$ decay has been reported [5]. Up to now, such hidden-charm pentaquark resonances have been observed only in the $J/\psi p$ and $J/\psi \Lambda$ systems. Investigation of such resonances in other decay modes, such as $\eta_c p$, $\chi_{c1} p$ and $\chi_{c2} p$ could shed light on the nature of these exotic states.

The partial widths of the $\Lambda_b^0 \to \chi_{c1} p K^-$ and $\Lambda_b^0 \to \chi_{c2} p K^-$ decays are measured to be almost equal [6]. For beauty mesons a different pattern is observed. The known partial widths for the $B \to \chi_{c1} K^{(*)}$ and the $B \to \chi_{c2} K^{(*)}$ decays [7–9] exhibit a large suppression of the decay modes with the χ_{c2} state with respect to the χ_{c1} state. Such suppression agrees with expectations from QCD factorisation [10]. More information on the decays of beauty baryons to the χ_{c1} and χ_{c2} states is needed to clarify the role of QCD factorisation in baryon decays.

In this paper, a search for the $\Lambda_b^0 \to \chi_{c1} p \pi^-$ and $\Lambda_b^0 \to \chi_{c2} p \pi^-$ decays is reported, where the χ_{c1} and χ_{c2} mesons are reconstructed via their radiative decays $\chi_{c1,2} \to J/\psi \gamma$, and the J/ψ mesons are reconstructed in the $\mu^+\mu^-$ final state. The $\Lambda_b^0 \to \chi_{c1} p K^-$ decay mode, which has a similar topology, is used as normalisation channel. The study is based on proton-proton (pp) collision data, corresponding to an integrated luminosity of $6\,\text{fb}^{-1}$, collected with the LHCb detector at a centre-of-mass energy of 13 TeV. Throughout this paper the inclusion of charge-conjugated processes is implied and the symbol χ_{cJ} is used to denote the χ_{c1} and χ_{c2} states collectively.

JHEP05(2021)095

2 Detector and simulation

The LHCb detector [11, 12] is a single-arm forward spectrometer covering the pseudorapidity range $2 < \eta < 5$, designed for the study of particles containing b or c quarks. The detector includes a high-precision tracking system consisting of a silicon-strip vertex detector surrounding the pp interaction region, a large-area silicon-strip detector located upstream of a dipole magnet with a bending power of about 4 Tm, and three stations of silicon-strip detectors and straw drift tubes placed downstream of the magnet. The tracking system provides a measurement of the momentum, p, of charged particles with a relative uncertainty that varies from 0.5% at low momentum to 1.0% at 200 GeV/c. The minimum distance of a track to a primary pp collision vertex (PV), the impact parameter (IP), is measured with a resolution of $(15 + 29/p_{\mathrm{T}})$ μm, where p_{T} is the component of the momentum transverse to the beam, in GeV/c. Different types of charged hadrons are distinguished using information from two ring-imaging Cherenkov (RICH) detectors. Photons, electrons and hadrons are identified by a calorimeter system consisting of scintillating-pad and preshower detectors, an electromagnetic and a hadronic calorimeter [13]. Muons are identified by a system composed of alternating layers of iron and multiwire proportional chambers.

The online event selection is performed by a trigger, which consists of a hardware stage, based on information from the calorimeter and muon systems, followed by a software stage, which applies a full event reconstruction. At the hardware trigger stage, events are required to have a muon with high transverse momentum or dimuon candidates in which a product of the p_{T} of the muons has a high value. In the software trigger, two oppositely charged muons are required to form a good-quality vertex that is significantly displaced from every PV, with a dimuon mass exceeding 2.7 GeV/c^2.

Simulated events are used to describe signal shapes and to compute the efficiencies needed to determine the branching fraction ratios. In the simulation, pp collisions are generated using Pythia [14] with a specific LHCb configuration [15]. Decays of unstable particles are described by EvtGen [16], in which final-state radiation is generated using Photos [17]. The interaction of the generated particles with the detector, and its response, are implemented using the Geant4 toolkit [18, 19] as described in ref. [20]. The transverse momentum and rapidity spectra of the Λ_{b}^0 baryons in simulated samples are adjusted to match those observed in a high-yield low-background sample of reconstructed $\Lambda_{\mathrm{b}}^0 \to \mathrm{J/\psi pK^-}$ decays. In the simulation, the Λ_{b}^0 baryon decays are produced according to a phase space decay model. Simulated $\Lambda_{\mathrm{b}}^0 \to \chi_{\mathrm{cJ}}\mathrm{pK^-}$ decays are corrected to reproduce the $\mathrm{pK^-}$ mass and $\cos\theta_{\mathrm{pK^-}}$ distributions observed in data, where $\theta_{\mathrm{pK^-}}$ is the helicity angle of the $\mathrm{pK^-}$ system, defined as the angle between the momentum vectors of the kaon and the Λ_{b}^0 baryon in the $\mathrm{pK^-}$ rest frame. Large calibration samples of low-background decays $\mathrm{D}^{*+} \to (\mathrm{D}^0 \to \mathrm{K^-}\pi^+)\,\pi^+$, $\mathrm{K_S^0} \to \pi^+\pi^-$, $\mathrm{D_s^+} \to (\phi \to \mathrm{K^+K^-})\,\pi^+$, $\Lambda \to \mathrm{p}\pi^-$ and $\Lambda_{\mathrm{c}}^+ \to \mathrm{pK^-}\pi^+$ [21, 22] are used to resample the combined detector response used for the identification of protons, kaons and pions. To account for imperfections in the simulation of charged-particle reconstruction, the track reconstruction efficiency determined from simulation is corrected using control channels in data [23].

JHEP05(2021)095

3 Event selection

The signal $\Lambda_b^0 \to \chi_{cJ} p\pi^-$ and the normalisation $\Lambda_b^0 \to \chi_{cJ} pK^-$ decays are both reconstructed using the decay modes $\chi_{cJ} \to J/\psi\gamma$ and $J/\psi \to \mu^+\mu^-$. A loose preselection similar to that used in refs. [9, 24–27] is applied, followed by a multivariate classifier based on a decision tree with gradient boosting (BDTG) [28].

Muon, proton, pion and kaon candidates are identified combining information from the RICH, calorimeter and muon detectors. They are required to have transverse momenta larger than 550, 500, 200 and 200 MeV/c, respectively. To ensure efficient particle identification, kaons and pions are required to have a momentum between 3.2 and 150 GeV/c, whilst protons must have momentum between 10 and 150 GeV/c. To reduce the combinatorial background due to particles produced in pp interactions, only tracks that are inconsistent with originating from any PV are used.

Pairs of oppositely charged muons consistent with originating from a common vertex are combined to form $J/\psi \to \mu^+\mu^-$ candidates. The transverse momentum of the dimuon candidate is required to be in excess of 2 GeV/c, and the mass of the $\mu^+\mu^-$ system is required to be between 3.020 and 3.135 GeV/c^2, where the asymmetric mass range around the known J/ψ mass [29] is chosen to account for final-state radiation. The position of the reconstructed dimuon vertex is required to be inconsistent with that of any reconstructed PV.

To create χ_{cJ} candidates, the selected J/ψ candidates are combined with photon candidates that have been reconstructed using clusters in the electromagnetic calorimeter. Only clusters that are not matched to the trajectory of a track extrapolated from the tracking system to the cluster position in the electromagnetic calorimeter are used in the analysis [13]. The transverse energies of the photon candidates are required to exceed 400 MeV. To suppress the large combinatorial background from $\pi^0 \to \gamma\gamma$ decays, photons that can form a $\pi^0 \to \gamma\gamma$ candidate with mass within 25 MeV/c^2 of the known π^0 mass [29] are ignored [30, 31]. The χ_{cJ} candidates are selected in the J/$\psi\gamma$ mass region between 3.4 and 3.7 GeV/c^2.

The selected χ_{cJ} candidates are combined with $p\pi^-$ or pK^- pairs to create $\Lambda_b^0 \to \chi_{cJ} p\pi^-$ or $\Lambda_b^0 \to \chi_{cJ} pK^-$ candidates, respectively. A kinematic fit [32] that constrains the four charged final-state particles to form a common vertex, the mass of the $\mu^+\mu^-$ combination to equal the known J/ψ mass [29] and the Λ_b^0 candidate to originate from the associated PV, is performed. Each Λ_b^0 candidate is associated with the PV that yields the smallest χ^2_{IP}, where χ^2_{IP} is defined as the difference in the vertex-fit χ^2 of a given PV reconstructed with and without the particle under consideration. A good-quality fit is required to further suppress combinatorial background. In addition, the measured decay time of the Λ_b^0 candidate, calculated with respect to the associated PV, is required to be greater than 0.1 mm/c to suppress poorly reconstructed candidates and background from particles originating directly from the PV.

To suppress cross-feed from $B^0 \to \chi_{cJ} K^+\pi^-$ decays with the positively charged kaon (negatively charged pion) misidentified as a proton (antiproton) for the signal (normalisation) channel, the Λ_b^0 candidate mass recalculated with a kaon (pion) mass

JHEP05(2021)095

hypothesis for the proton is required to be inconsistent with the known B^0 meson mass [29]. In a similar way, Λ_b^0 candidates are rejected if the mass of the $p\pi^-$ (pK^-) combination is consistent with the known ϕ-meson mass [29] when a kaon mass hypothesis is used for both hadrons. To suppress background from the $\Lambda \to p\pi^-$ decay, candidates with a $p\pi^-$ mass that is consistent with the known mass of the Λ baryon [29] are rejected. The contributions from the $\Lambda_b^0 \to J/\psi p\pi^-$ and $\Lambda_b^0 \to J/\psi pK^-$ decays combined with random photons are eliminated by the requirement that the mass of the Λ_b^0 candidate calculated without a photon is inconsistent with the known mass of the Λ_b^0 baryon [6, 29]. Finally, the contributions from wrongly reconstructed $B^0 \to J/\psi K^+\pi^-$, $\Lambda_b^0 \to J/\psi pK^-$ and $B_s^0 \to J/\psi K^+K^-$ decays, combined with random photons, are rejected by the requirement that the mass of the Λ_b^0 candidate recalculated using different mass hypotheses for the pion, kaon and proton candidates and ignoring the photon in the final state, be inconsistent with the known mass of the corresponding beauty hadron.

To suppress a potentially large combinatorial background, separate BDTG classifiers are used for the $\Lambda_b^0 \to \chi_{cJ} p\pi^-$ and $\Lambda_b^0 \to \chi_{cJ} pK^-$ candidates. The BDTG classifier for the $\Lambda_b^0 \to \chi_{cJ} p\pi^-$ ($\Lambda_b^0 \to \chi_{cJ} pK^-$) candidates is trained on simulated samples of $\Lambda_b^0 \to \chi_{c1} p\pi^-$ ($\Lambda_b^0 \to \chi_{c1} pK^-$) decays for the signal and candidates from data with $\chi_{c1} p\pi^-$ ($\chi_{c1} pK^-$) mass between 5.65 and 6.00 GeV/c^2 for the background. The k-fold cross-validation technique [33] with $k = 7$ is used to avoid introducing a bias in the BDTG output. The BDTG classifier for the $\Lambda_b^0 \to \chi_{cJ} p\pi^-$ ($\Lambda_b^0 \to \chi_{cJ} pK^-$) candidates is trained on variables related to the reconstruction quality, kinematics and decay time of Λ_b^0 candidates, kinematics of particles in the final state and the estimated probabilities that protons and pions (kaons) are correctly identified by the particle identification detectors [21, 22]. The requirement on the BDTG output is chosen to maximize the figure-of-merit $S/\sqrt{S+B}$, where S and B are expected signal and background yields, correspondingly. The signal yields are estimated from the simulated samples, normalised to the signal yields observed in data for the loose requirements on the BDTG output, and the background yield B is estimated from the fit to data using a model, described in section 4.

After application of the BDTG requirement, 6% of events with $\Lambda_b^0 \to \chi_{cJ} p\pi^-$ candidates in the $5.4 < m_{\chi_{c1}p\pi^-} < 5.8$ GeV/c^2 region and 13% of events with $\Lambda_b^0 \to \chi_{cJ} pK^-$ candidates in the $5.3 < m_{\chi_{c1}pK^-} < 5.8$ GeV/c^2 region contain multiple candidates. These multiple candidates are predominantly caused by the $J/\psi p\pi^-$ or $J/\psi pK^-$ combination being combined with different photons in the event. A study using simulation shows that the random photons causing multiple candidates typically have lower transverse energy with respect to that of the photons originating from the Λ_b^0 baryon decay. Therefore, to reduce multiple candidates for each event, only the Λ_b^0 candidate with the highest transverse energy photon is retained.

To improve the Λ_b^0 mass resolution, the mass of the Λ_b^0 candidates is calculated using a kinematic fit [32], similar to the one described above, but with an additional constraint fixing the mass of the $J/\psi\gamma$ combination to the known χ_{c1} mass [29]. For the $\Lambda_b^0 \to \chi_{c1} p\pi^-$ and $\Lambda_b^0 \to \chi_{c1} pK^-$ decays, the mass calculated with such a constraint forms a narrow peak at the known mass of the Λ_b^0 baryon, while for the $\Lambda_b^0 \to \chi_{c2} p\pi^-$ and $\Lambda_b^0 \to \chi_{c2} pK^-$ decays the narrow peak is shifted towards lower values [6, 9].

JHEP05(2021)095

4 Signal yields and efficiencies

The mass distributions for selected $\Lambda_b^0 \to \chi_{cJ} p\pi^-$ and $\Lambda_b^0 \to \chi_{cJ} pK^-$ candidates are shown in figures 1 and 2, respectively. The signal yields are determined using unbinned extended maximum-likelihood fits to these distributions. For the $\Lambda_b^0 \to \chi_{cJ} p\pi^-$ channel, the fit model consists of two signal components, corresponding to the $\Lambda_b^0 \to \chi_{c1} p\pi^-$ and $\Lambda_b^0 \to \chi_{c2} p\pi^-$ decays, as described below, and a combinatorial background component that is described by the product of an exponential function and a first-order polynomial function, required to be positive in the relevant mass range. For the $\Lambda_b^0 \to \chi_{cJ} pK^-$ channel, the fit model consists of two signal components, corresponding to the $\Lambda_b^0 \to \chi_{c1} pK^-$ and $\Lambda_b^0 \to \chi_{c2} pK^-$ decays, a combinatorial background component which is described by a concave third-order positive polynomial function and a component from partially reconstructed Λ_b^0 baryon decays, such as $\Lambda_b^0 \to \psi(2S) pK^-$ with subsequent decays $\psi(2S) \to J/\psi\pi\pi$, $\psi(2S) \to J/\psi\eta$ or $\psi(2S) \to (\chi_{c1} \to J/\psi\gamma)\gamma$, which is described by a Gaussian function. Each of the four signal components is described by the sum of two Crystal Ball (CB) functions [34] with a common mean and power-law tails on both sides. The tail parameters of the CB functions, the ratio of the widths of the two CB functions, and their relative normalisation are fixed to the values obtained from simulation. The widths and the difference in the mean values for the large $\Lambda_b^0 \to \chi_{c1} pK^-$ and $\Lambda_b^0 \to \chi_{c2} pK^-$ components are allowed to vary in the fit, while for the small $\Lambda_b^0 \to \chi_{c1} p\pi^-$ and $\Lambda_b^0 \to \chi_{c2} p\pi^-$ components, the difference in the mean values and the ratio of widths are constrained to the values obtained from simulation.

The signal yields for the $\Lambda_b^0 \to \chi_{c1} p\pi^-$, $\Lambda_b^0 \to \chi_{c2} p\pi^-$, $\Lambda_b^0 \to \chi_{c1} pK^-$ and $\Lambda_b^0 \to \chi_{c2} pK^-$ decay modes are summarized in table 1. The statistical significance for the $\Lambda_b^0 \to \chi_{c1} p\pi^-$ and $\Lambda_b^0 \to \chi_{c2} p\pi^-$ fit components is estimated using Wilks' theorem [35]. The significance for the $\Lambda_b^0 \to \chi_{c2} p\pi^-$ signal is confirmed by simulating a large number of pseudoexperiments according to the background distributions observed in data. The statistical significance is found to be 9.6 and 3.8 standard deviations for the $\Lambda_b^0 \to \chi_{c1} p\pi^-$ and $\Lambda_b^0 \to \chi_{c2} p\pi^-$ decay modes, respectively.

The measured yields for the $\Lambda_b^0 \to \chi_{c1} p\pi^-$, $\Lambda_b^0 \to \chi_{c2} p\pi^-$, $\Lambda_b^0 \to \chi_{c1} pK^-$ and $\Lambda_b^0 \to \chi_{c2} pK^-$ decay modes are used to calculate the ratios of branching fractions

$$\mathcal{R}_{\pi/K} \equiv \frac{\mathcal{B}\left(\Lambda_b^0 \to \chi_{c1} p\pi^-\right)}{\mathcal{B}\left(\Lambda_b^0 \to \chi_{c1} pK^-\right)} = \frac{N_{\Lambda_b^0 \to \chi_{c1} p\pi^-}}{N_{\Lambda_b^0 \to \chi_{c1} pK^-}} \times \frac{\varepsilon_{\Lambda_b^0 \to \chi_{c1} pK^-}}{\varepsilon_{\Lambda_b^0 \to \chi_{c1} p\pi^-}}, \tag{4.1a}$$

$$\mathcal{R}^{\pi}_{2/1} \equiv \frac{\mathcal{B}\left(\Lambda_b^0 \to \chi_{c2} p\pi^-\right)}{\mathcal{B}\left(\Lambda_b^0 \to \chi_{c1} p\pi^-\right)} = \frac{N_{\Lambda_b^0 \to \chi_{c2} p\pi^-}}{N_{\Lambda_b^0 \to \chi_{c1} p\pi^-}} \times \frac{\varepsilon_{\Lambda_b^0 \to \chi_{c1} p\pi^-}}{\varepsilon_{\Lambda_b^0 \to \chi_{c2} p\pi^-}} \times \frac{\mathcal{B}(\chi_{c1} \to J/\psi\gamma)}{\mathcal{B}(\chi_{c2} \to J/\psi\gamma)}, \tag{4.1b}$$

$$\mathcal{R}^{K}_{2/1} \equiv \frac{\mathcal{B}\left(\Lambda_b^0 \to \chi_{c2} pK^-\right)}{\mathcal{B}\left(\Lambda_b^0 \to \chi_{c1} pK^-\right)} = \frac{N_{\Lambda_b^0 \to \chi_{c2} pK^-}}{N_{\Lambda_b^0 \to \chi_{c1} pK^-}} \times \frac{\varepsilon_{\Lambda_b^0 \to \chi_{c1} pK^-}}{\varepsilon_{\Lambda_b^0 \to \chi_{c2} pK^-}} \times \frac{\mathcal{B}(\chi_{c1} \to J/\psi\gamma)}{\mathcal{B}(\chi_{c2} \to J/\psi\gamma)}, \tag{4.1c}$$

where N stands for the measured yield, ε denotes the efficiency of the corresponding decay and $\mathcal{B}(\chi_{cJ} \to J/\psi\gamma)$ are the branching fractions of the radiative $\chi_{cJ} \to J/\psi\gamma$ decays, taken from ref. [29]. The efficiency is defined as the product of the detector acceptance, reconstruction, selection and trigger efficiencies, where each subsequent efficiency is defined with respect to the previous one. Each of the partial efficiencies is calculated using the appropriately corrected simulation samples. The efficiencies are determined separately for each

JHEP05(2021)095

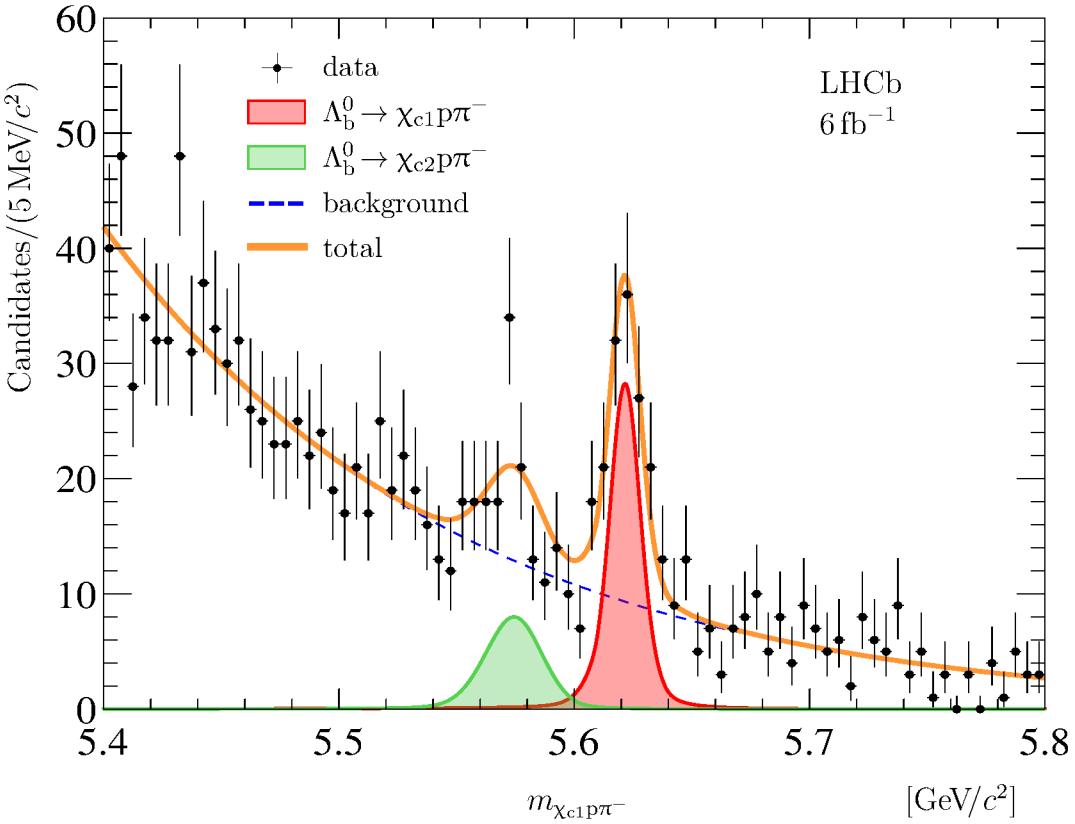

Figure 1. Mass distribution for selected $\Lambda_b^0 \to \chi_{cJ} p\pi^-$ candidates. A fit, described in the text, is overlaid.

data-taking period and are combined according to the corresponding luminosity for each period. The ratios of the total efficiencies are determined to be

$$\frac{\varepsilon_{\Lambda_b^0 \to \chi_{c1} pK^-}}{\varepsilon_{\Lambda_b^0 \to \chi_{c1} p\pi^-}} = 1.969 \pm 0.008\,, \tag{4.2a}$$

$$\frac{\varepsilon_{\Lambda_b^0 \to \chi_{c1} p\pi^-}}{\varepsilon_{\Lambda_b^0 \to \chi_{c2} p\pi^-}} = 1.088 \pm 0.007\,, \tag{4.2b}$$

$$\frac{\varepsilon_{\Lambda_b^0 \to \chi_{c1} pK^-}}{\varepsilon_{\Lambda_b^0 \to \chi_{c2} pK^-}} = 1.043 \pm 0.007\,, \tag{4.2c}$$

where only the uncertainty that arises from the sizes of the simulated samples is given. The $\Lambda_b^0 \to \chi_{c1} p\pi^-$ decay channel has a much higher combinatorial background level, therefore, the BDTG selection is less efficient with respect to that for the $\Lambda_b^0 \to \chi_{c1} pK^-$ channel, which is the main factor causing the difference in total efficiencies for these channels. Using these ratios of efficiencies and the measured yields from table 1, the ratios of the branching fractions are found to be

$$\begin{aligned} \mathcal{R}_{\pi/K} &= (6.59 \pm 1.01) \times 10^{-2}\,, \\ \mathcal{R}^{\pi}_{2/1} &= 0.95 \pm 0.30\,, \\ \mathcal{R}^{K}_{2/1} &= 1.06 \pm 0.05\,, \end{aligned}$$

JHEP05(2021)095

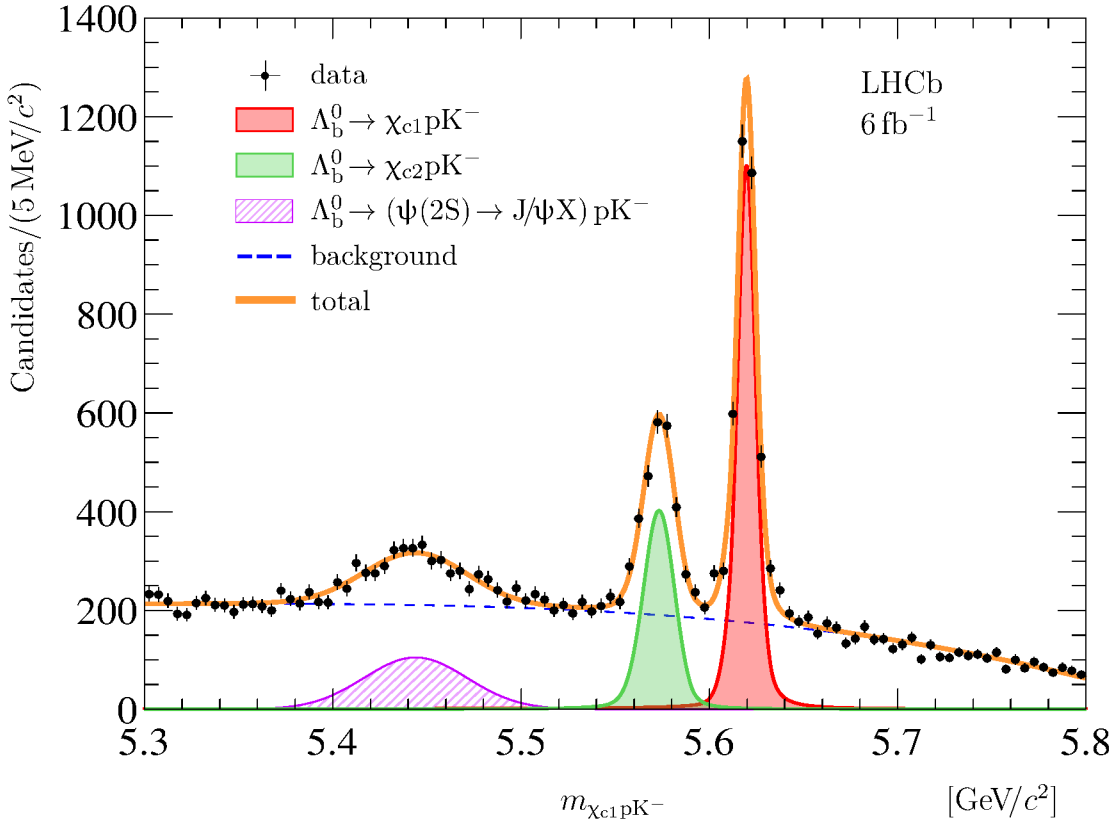

Figure 2. Mass distribution for selected $\Lambda_b^0 \to \chi_{cJ} pK^-$ candidates. A fit, described in the text, is overlaid.

Decay mode	N
$\Lambda_b^0 \to \chi_{c1} p\pi^-$	105 ± 16
$\Lambda_b^0 \to \chi_{c2} p\pi^-$	51 ± 16
$\Lambda_b^0 \to \chi_{c1} pK^-$	3133 ± 75
$\Lambda_b^0 \to \chi_{c2} pK^-$	1766 ± 71

Table 1. Signal yields, N, from the fits described in the text. The uncertainties are statistical only.

where the uncertainties are statistical only. Systematic uncertainties are discussed in the next section.

Background-subtracted $\chi_{c1}p$, $\chi_{c1}\pi^-$ and $p\pi^-$ mass distributions from the $\Lambda_b^0 \to \chi_{c1} p\pi^-$ decay are shown in figure 3. The *sPlot* technique, with the $\chi_{c1} p\pi^-$ mass as the discriminating variable, is used for background subtraction [36]. The distributions are compared with those obtained from simulated decays generated according to a phase space model and, with the present dataset, no evidence for large contributions from possible exotic states is found.

JHEP05(2021)095

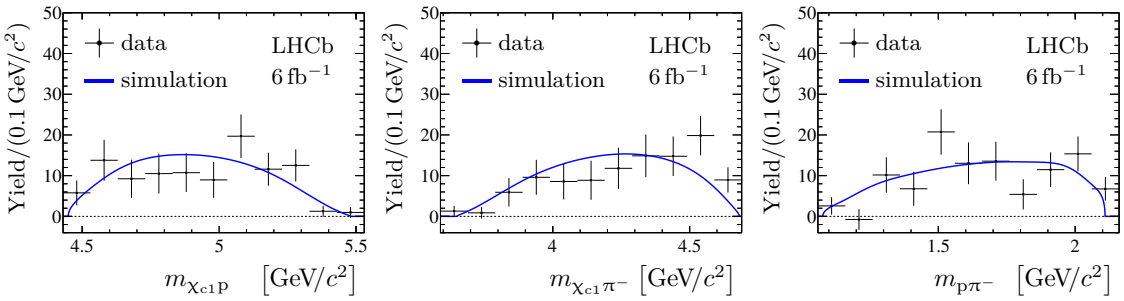

Figure 3. Background-subtracted mass distributions of the (left) $\chi_{c1}p$, (centre) $\chi_{c1}\pi^-$ and (right) $p\pi^-$ combinations in the $\Lambda_b^0 \to \chi_{c1}p\pi^-$ decay. Expectations from a phase space simulation are overlaid.

5 Systematic uncertainties

Since the $\Lambda_b^0 \to \chi_{cJ}p\pi^-$ and $\Lambda_b^0 \to \chi_{cJ}pK^-$ decay channels have similar kinematics and topologies, systematic uncertainties largely cancel in the ratios $\mathcal{R}$ defined by eqs. (4.1). The remaining contributions to the systematic uncertainties are summarized in table 2 and discussed below.

The systematic uncertainty related to the signal and background shapes is investigated using alternative parameterisations. For the $\Lambda_b^0 \to \chi_{c1}p\pi^-$ and $\Lambda_b^0 \to \chi_{c1}pK^-$ components, two alternative models are probed. The first model consists of a sum of a Student's t-distribution [37] and a double-sided Crystal Ball function (CB_2) with power-law tails on both sides of the peak [38]. The second alternative model is a sum of a Gaussian and CB_2 functions. For the $\Lambda_b^0 \to \chi_{c2}p\pi^-$ and $\Lambda_b^0 \to \chi_{c2}pK^-$ components, two other alternative models are probed: a sum of a bifurcated Student's t-distribution with a CB_2 function, and a sum of a skewed Gaussian function [39] with a CB_2 function. The alternative parameterisations for the component from partially reconstructed Λ_b^0 decays include a bifurcated Gaussian function and a Student's t-distribution. Two alternative shapes are used for the background parameterisation. The first model consists of a product of an exponential function and a second-order positive polynomial function, while a fourth-order concave positive polynomial function is used as the second alternative model. The systematic uncertainty related to the fit model is estimated by producing pseudoexperiments generated with the baseline fit model and fitted with alternative models. Each pseudoexperiment is approximately 100 times larger than the data sample. The maximal deviations for the ratios of the signal yields with respect to the baseline model are taken as systematic uncertainties in the ratios $\mathcal{R}$. The assigned systematic uncertainties are 2.4%, 3.7% and 3.7% in the ratios $\mathcal{R}_{\pi/K}$, $\mathcal{R}^{\pi}_{2/1}$ and $\mathcal{R}^{K}_{2/1}$, respectively.

An additional systematic uncertainty in the ratios $\mathcal{R}$ arises due to differences between data and simulation. The transverse momentum and rapidity spectra of the Λ_b^0 baryons in simulated samples are adjusted to match those observed in a high-yield low-background sample of reconstructed $\Lambda_b^0 \to J/\psi pK^-$ decays. The finite size of this sample causes uncertainty in the obtained Λ_b^0 production spectra. The systematic uncertainty in the efficiency ratios, related to the imprecise knowledge of the production Λ_b^0 baryon spectra is estimated

JHEP05(2021)095

Source	$\mathcal{R}_{\pi/\mathrm{K}}$	$\mathcal{R}^{\pi}_{2/1}$	$\mathcal{R}^{\mathrm{K}}_{2/1}$
Fit model	2.4	3.7	3.7
Λ_{b}^0 production spectra	< 0.1		
$\Lambda_{\mathrm{b}}^0 \to \chi_{\mathrm{cJ}}\mathrm{pK}^-$ decay models	< 0.1		< 0.1
Track reconstruction	< 0.1		
Hadron identification	0.3		
Trigger efficiency	1.1		
BDTG selection	2.0		
Simulation sample size	0.4	0.6	0.7
Total	3.3	3.8	3.8

Table 2. Relative systematic uncertainties (in %) in the ratios of branching fractions. The total uncertainty is obtained as the sum of individual components in quadrature. Empty cells correspond to cases where no uncertainty is applicable.

using the variation of the kinematic spectra of the selected $\Lambda_{\mathrm{b}}^0 \to \mathrm{J/\psi pK}^-$ sample within their statistical uncertainty. This systematic uncertainty is found to be smaller than 0.1% in the $\mathcal{R}_{\pi/\mathrm{K}}$ ratio and even smaller for the $\mathcal{R}^{\pi}_{2/1}$ and $\mathcal{R}^{\mathrm{K}}_{2/1}$ ratios.

The simulated $\Lambda_{\mathrm{b}}^0 \to \chi_{\mathrm{cJ}}\mathrm{pK}^-$ decays are corrected to reproduce the pK^- mass and $\cos\theta_{\mathrm{pK}^-}$ distributions observed in data. The systematic uncertainty in the $\varepsilon_{\Lambda_{\mathrm{b}}^0 \to \chi_{\mathrm{c1}}\mathrm{pK}^-}$ and $\varepsilon_{\Lambda_{\mathrm{b}}^0 \to \chi_{\mathrm{c2}}\mathrm{pK}^-}$ efficiencies, related to the imprecise knowledge of the decay model for the $\Lambda_{\mathrm{b}}^0 \to \chi_{\mathrm{cJ}}\mathrm{pK}^-$ decays, is estimated using the variation of the pK^- mass and $\cos\theta_{\mathrm{pK}^-}$ spectra within their uncertainties. The corresponding systematic uncertainties in the $\mathcal{R}_{\pi/\mathrm{K}}$ and $\mathcal{R}^{\mathrm{K}}_{2/1}$ ratios are found to be less than 0.1%.

There are residual differences in the reconstruction efficiency of charged-particle tracks that do not cancel completely in the ratio due to the different kinematic distributions of the final-state particles. The track-finding efficiencies obtained from simulated samples are corrected using calibration channels [23]. The uncertainties related to the efficiency correction factors, are propagated to the ratios of the total efficiencies using pseudoexperiments and found to be smaller than 0.1% in the ratio $\mathcal{R}_{\pi/\mathrm{K}}$ and smaller in the ratios $\mathcal{R}^{\pi}_{2/1}$ and $\mathcal{R}^{\mathrm{K}}_{2/1}$. A small difference between data and simulation for the photon reconstruction is studied using a large sample of $\mathrm{B}^+ \to \mathrm{J/\psi}\,(\mathrm{K}^{*+} \to \mathrm{K}^+\,(\pi^0 \to \gamma\gamma))$ decays [30, 40, 41] The associated systematic uncertainty largely cancels in the ratios $\mathcal{R}$.

The combined detector response used for the identification of protons, kaons and pions in simulation is resampled from control channels [22]. The systematic uncertainty obtained through this procedure arises from the kernel shape used in the estimation of the probability density distributions. An alternative combined response is estimated using an alternative kernel estimation with a changed shape and the efficiency models are regenerated [42, 43]. The difference between the two estimates for the efficiency ratios is taken as the systematic uncertainty related to hadron identification and is found to be 0.3% in the ratio $\mathcal{R}_{\pi/\mathrm{K}}$. In the ratios $\mathcal{R}^{\pi}_{2/1}$ and $\mathcal{R}^{\mathrm{K}}_{2/1}$ this systematic uncertainty cancels as it is assumed to be fully correlated between the modes with χ_{c1} and χ_{c2} mesons.

JHEP05(2021)095

A systematic uncertainty in the ratios related to the knowledge of the trigger efficiencies has been previously studied using high-yield $B^+ \to J/\psi K^+$ and $B^+ \to \psi(2S)K^+$ decays by comparing ratios of trigger efficiencies in data and simulation [44]. Based on these comparisons, a relative uncertainty of 1.1% is assigned to $\mathcal{R}_{\pi/K}$, while for $\mathcal{R}^{\pi}_{2/1}$ and $\mathcal{R}^{K}_{2/1}$ it is expected to cancel in the ratio due to resemblance of the kinematics of the corresponding decay channels.

The imperfect data description by the simulation due to remaining effects is studied by varying the BDTG selection criteria in ranges that lead to ±20% changes in the measured efficiency. For this study, the high-statistics normalisation channel is used. The resulting difference between the efficiency estimated using data and simulation does not exceed 2.0%, which is taken as a systematic uncertainty in $\mathcal{R}_{\pi/K}$. This systematic uncertainty in $\mathcal{R}^{\pi}_{2/1}$ and $\mathcal{R}^{K}_{2/1}$ is considered negligible due to the similarity of the kinematics of the corresponding decay channels.

Finally, the uncertainties in the ratios of efficiencies from eqs. (4.2) are 0.4%, 0.6% and 0.7% and are taken as systematic uncertainties due to the finite size of the simulated samples for the $\mathcal{R}_{\pi/K}$, $\mathcal{R}^{\pi}_{2/1}$ and $\mathcal{R}^{K}_{2/1}$, respectively.

For each choice of the fit model, the statistical significance of the $\Lambda_b^0 \to \chi_{c2} p\pi^-$ signal is calculated from data using Wilks' theorem [35] and confirmed by simulating a large number of pseudoexperiments. The smallest significance found is 3.5 standard deviations, taken as its significance including systematic uncertainties.

6 Results and summary

A search for the Cabibbo-suppressed decays $\Lambda_b^0 \to \chi_{cJ} p\pi^-$ is performed using a data sample collected by the LHCb experiment in proton-proton collisions at a centre-of-mass energy of 13 TeV and corresponding to $6\,\text{fb}^{-1}$ of integrated luminosity. The $\Lambda_b^0 \to \chi_{c1} p\pi^-$ decay is observed for the first time with a yield of 105 ± 16 and a statistical significance above 9 standard deviations. First evidence for the $\Lambda_b^0 \to \chi_{c2} p\pi^-$ decay is obtained with a yield of 51 ± 16 and a significance of 3.5 standard deviations. The ratios of the branching fractions are measured to be

$$\mathcal{R}_{\pi/K} = \frac{\mathcal{B}(\Lambda_b^0 \to \chi_{c1} p\pi^-)}{\mathcal{B}(\Lambda_b^0 \to \chi_{c1} pK^-)} = (6.59 \pm 1.01 \pm 0.22) \times 10^{-2}\,,$$

$$\mathcal{R}^{\pi}_{2/1} = \frac{\mathcal{B}(\Lambda_b^0 \to \chi_{c2} p\pi^-)}{\mathcal{B}(\Lambda_b^0 \to \chi_{c1} p\pi^-)} = 0.95 \pm 0.30 \pm 0.04 \pm 0.04\,,$$

$$\mathcal{R}^{K}_{2/1} = \frac{\mathcal{B}(\Lambda_b^0 \to \chi_{c2} pK^-)}{\mathcal{B}(\Lambda_b^0 \to \chi_{c1} pK^-)} = 1.06 \pm 0.05 \pm 0.04 \pm 0.04\,,$$

where the first uncertainty is statistical, the second is systematic and the third is related to the uncertainties in the branching fractions of the $\chi_{cJ} \to J/\psi\gamma$ decays [29]. The ratio $\mathcal{R}_{\pi/K}$ is similar to analogous ratios for other Cabibbo-suppressed decays of the Λ_b^0 baryon [26, 45]. The expected value for the ratio $\mathcal{R}_{\pi/K}$, if neglecting the resonance structures in the $\Lambda_b^0 \to \chi_{c1} p\pi^-$ and $\Lambda_b^0 \to \chi_{c1} pK^-$ decays, is

$$\frac{\Phi_3(\Lambda_b^0 \to \chi_{c1} p\pi^-)}{\Phi_3(\Lambda_b^0 \to \chi_{c1} pK^-)} \times \tan^2\theta_C \simeq 9.9\%\,,$$

JHEP05(2021)095

where Φ_3 denotes the full three-body phase space and θ_C is the Cabibbo angle [46]. The ratio $\mathcal{R}^{K}_{2/1}$ agrees well with the previous measurement by the LHCb collaboration of $1.02 \pm 0.10 \pm 0.02 \pm 0.05$ [6]. This result has better precision and arises from a statistically independent sample from that of ref. [6]. Similarly to $\mathcal{R}^{K}_{2/1}$, the new result for $\mathcal{R}^{\pi}_{2/1}$ shows no suppression of the χ_{c2} mode relative to the χ_{c1} mode, which challenges the factorisation approach for Λ_b^0 decays [10].

The background-subtracted $\chi_{c1}p$ and $\chi_{c1}\pi^-$ mass distributions for the $\Lambda_b^0 \to \chi_{c1}p\pi^-$ decay are investigated. With the present dataset, the results are consistent with a phase space model, and no evidence for contributions from exotic states is found.

Acknowledgments

We express our gratitude to our colleagues in the CERN accelerator departments for the excellent performance of the LHC. We thank the technical and administrative staff at the LHCb institutes. We acknowledge support from CERN and from the national agencies: CAPES, CNPq, FAPERJ and FINEP (Brazil); MOST and NSFC (China); CNRS/IN2P3 (France); BMBF, DFG and MPG (Germany); INFN (Italy); NWO (Netherlands); MNiSW and NCN (Poland); MEN/IFA (Romania); MSHE (Russia); MICINN (Spain); SNSF and SER (Switzerland); NASU (Ukraine); STFC (United Kingdom); DOE NP and NSF (U.S.A.). We acknowledge the computing resources that are provided by CERN, IN2P3 (France), KIT and DESY (Germany), INFN (Italy), SURF (Netherlands), PIC (Spain), GridPP (United Kingdom), RRCKI and Yandex LLC (Russia), CSCS (Switzerland), IFIN-HH (Romania), CBPF (Brazil), PL-GRID (Poland) and NERSC (U.S.A.). We are indebted to the communities behind the multiple open-source software packages on which we depend. Individual groups or members have received support from ARC and ARDC (Australia); AvH Foundation (Germany); EPLANET, Marie Skłodowska-Curie Actions and ERC (European Union); A*MIDEX, ANR, Labex P2IO and OCEVU, and Région Auvergne-Rhône-Alpes (France); Key Research Program of Frontier Sciences of CAS, CAS PIFI, CAS CCEPP, Fundamental Research Funds for the Central Universities, and Sci. & Tech. Program of Guangzhou (China); RFBR, RSF and Yandex LLC (Russia); GVA, XuntaGal and GENCAT (Spain); the Leverhulme Trust, the Royal Society and UKRI (United Kingdom).

JHEP05(2021)095

References

[1] LHCb collaboration, *Observation of* $J/\psi p$ *resonances consistent with pentaquark states in* $\Lambda_b^0 \to J/\psi p K^-$ *decays*, *Phys. Rev. Lett.* **115** (2015) 072001 [arXiv:1507.03414] [INSPIRE].

[2] LHCb collaboration, *Model-independent evidence for* $J/\psi p$ *contributions to* $\Lambda_b^0 \to J/\psi p K^-$ *decays*, *Phys. Rev. Lett.* **117** (2016) 082002 [arXiv:1604.05708] [INSPIRE].

[3] LHCb collaboration, *Observation of a narrow pentaquark state,* $P_c(4312)^+$*, and of two-peak structure of the* $P_c(4450)^+$, *Phys. Rev. Lett.* **122** (2019) 222001 [arXiv:1904.03947] [INSPIRE].

[4] LHCb collaboration, *Evidence for exotic hadron contributions to* $\Lambda_b^0 \to J/\psi p \pi^-$ *decays*, *Phys. Rev. Lett.* **117** (2016) 082003 [*Addendum ibid.* **117** (2016) 109902] [*Addendum ibid.* **118** (2017) 119901] [arXiv:1606.06999] [INSPIRE].

[5] LHCb collaboration, *Evidence of a* $J/\psi\Lambda$ *structure and observation of excited* Ξ^- *states in the* $\Xi_b^- \to J/\psi\Lambda K^-$ *decay*, arXiv:2012.10380 [INSPIRE].

[6] LHCb collaboration, *Observation of the decays* $\Lambda_b^0 \to \chi_{c1} p K^-$ *and* $\Lambda_b^0 \to \chi_{c2} p K^-$, *Phys. Rev. Lett.* **119** (2017) 062001 [arXiv:1704.07900] [INSPIRE].

[7] Belle collaboration, *Observation of two resonance-like structures in the* $\pi^+\chi_{c1}$ *mass distribution in exclusive* $\overline{B}^0 \to K^-\pi^+\chi_{c1}$ *decays*, *Phys. Rev. D* **78** (2008) 072004 [arXiv:0806.4098] [INSPIRE].

[8] BaBar collaboration, *Evidence for* $X(3872) \to \psi(2S)\gamma$ *in* $B^\pm \to X(3872)K^\pm$ *decays, and a study of* $B \to c\bar{c}\gamma K$, *Phys. Rev. Lett.* **102** (2009) 132001 [arXiv:0809.0042] [INSPIRE].

[9] LHCb collaboration, *Observation of* $B_s^0 \to \chi_{c1}\phi$ *decay and study of* $B^0 \to \chi_{c1,2} K^{*0}$ *decays*, *Nucl. Phys. B* **874** (2013) 663 [arXiv:1305.6511] [INSPIRE].

[10] M. Beneke and L. Vernazza, $B \to \chi_{cJ} K$ *decays revisited*, *Nucl. Phys. B* **811** (2009) 155 [arXiv:0810.3575] [INSPIRE].

[11] LHCb collaboration, *The LHCb detector at the LHC*, 2008 *JINST* **3** S08005 [INSPIRE].

[12] LHCb collaboration, *LHCb detector performance*, *Int. J. Mod. Phys. A* **30** (2015) 1530022 [arXiv:1412.6352] [INSPIRE].

[13] C. Abellán Beteta et al., *Calibration and performance of the LHCb calorimeters in Run 1 and 2 at the LHC*, arXiv:2008.11556 [INSPIRE].

[14] T. Sjöstrand, S. Mrenna and P.Z. Skands, *A brief introduction to* Pythia 8.1, *Comput. Phys. Commun.* **178** (2008) 852 [arXiv:0710.3820] [INSPIRE].

[15] I. Belyaev et al., *Handling of the generation of primary events in* Gauss, *the LHCb simulation framework*, *J. Phys. Conf. Ser.* **331** (2011) 032047 [INSPIRE].

[16] D.J. Lange, *The* EvtGen *particle decay simulation package*, *Nucl. Instrum. Meth. A* **462** (2001) 152 [INSPIRE].

[17] N. Davidson, T. Przedzinski and Z. Was, Photos *interface in C++: Technical and physics documentation*, *Comput. Phys. Commun.* **199** (2016) 86 [arXiv:1011.0937] [INSPIRE].

JHEP05(2021)095

[18] GEANT4 collaboration, GEANT4 *developments and applications*, *IEEE Trans. Nucl. Sci.* **53** (2006) 270 [INSPIRE].

[19] GEANT4 collaboration, GEANT4*: A simulation toolkit*, *Nucl. Instrum. Meth. A* **506** (2003) 250 [INSPIRE].

[20] M. Clemencic et al., *The LHCb simulation application,* GAUSS*: Design, evolution and experience*, *J. Phys. Conf. Ser.* **331** (2011) 032023 [INSPIRE].

[21] M. Adinolfi et al., *Performance of the LHCb RICH detector at the LHC*, *Eur. Phys. J. C* **73** (2013) 2431 [arXiv:1211.6759] [INSPIRE].

[22] R. Aaij et al., *Selection and processing of calibration samples to measure the particle identification performance of the LHCb experiment in Run 2*, *EPJ Tech. Instrum.* **6** (2019) 1 [arXiv:1803.00824] [INSPIRE].

[23] LHCb collaboration, *Measurement of the track reconstruction efficiency at LHCb*, 2015 *JINST* **10** P02007 [arXiv:1408.1251] [INSPIRE].

[24] LHCb collaboration, *Evidence for the decay* $X(3872) \to \psi(2S)\gamma$, *Nucl. Phys. B* **886** (2014) 665 [arXiv:1404.0275] [INSPIRE].

[25] LHCb collaboration, *Observation of* $\Lambda_b^0 \to \psi(2S)pK^-$ *and* $\Lambda_b^0 \to J/\psi\pi^+\pi^- pK^-$ *decays and a measurement of the* Λ_b^0 *baryon mass*, *JHEP* **05** (2016) 132 [arXiv:1603.06961] [INSPIRE].

[26] LHCb collaboration, *Observation of the decay* $\Lambda_b^0 \to \psi(2S)p\pi^-$, *JHEP* **08** (2018) 131 [arXiv:1806.08084] [INSPIRE].

[27] LHCb collaboration, *Observation of the* $\Lambda_b^0 \to \chi_{c2}(3872)pK^-$ *decay*, *JHEP* **09** (2019) 028 [arXiv:1907.00954] [INSPIRE].

[28] L. Breiman, J. Friedman, R.A. Olshen and C.J. Stone, *Classification and regression trees*, Wadsworth international group, Belmont, California, U.S.A. (1984).

[29] PARTICLE DATA GROUP collaboration, *Review of particle physics*, *PTEP* **2020** (2020) 083C01 [INSPIRE].

[30] LHCb collaboration, *Evidence for the decay* $B^0 \to J/\psi\omega$ *and measurement of the relative branching fractions of* B_s^0 *meson decays to* $J/\psi\eta$ *and* $J/\psi\eta'$, *Nucl. Phys. B* **867** (2013) 547 [arXiv:1210.2631] [INSPIRE].

[31] LHCb collaboration, *Study of* $\eta - \eta'$ *mixing from measurement of* $B_{(s)}^0 \to J/\psi\eta'$ *decay rates*, *JHEP* **01** (2015) 024 [arXiv:1411.0943] [INSPIRE].

[32] W.D. Hulsbergen, *Decay chain fitting with a Kalman filter*, *Nucl. Instrum. Meth. A* **552** (2005) 566 [physics/0503191] [INSPIRE].

[33] S. Geisser, *Predictive inference: An introduction*, Chapman and Hall/CRC, New York (1993) [DOI].

[34] T. Skwarnicki, *A study of the radiative cascade transitions between the* Υ' *and* Υ *resonances*, Ph.D. Thesis, Institute of Nuclear Physics, Krakow (1986) [DESY-F31-86-02].

[35] S.S. Wilks, *The large-sample distribution of the likelihood ratio for testing composite hypotheses*, Ann. Math. Stat. **9** (1938) 60.

[36] M. Pivk and F.R. Le Diberder, *sPlot: A statistical tool to unfold data distributions*, *Nucl. Instrum. Meth. A* **555** (2005) 356 [physics/0402083] [INSPIRE].

[37] Student (W.S. Gosset), *The probable error of a mean*, *Biometrika* **6** (1908) 1.

JHEP05(2021)095

[38] LHCb collaboration, *Observation of* J/ψ*-pair production in* pp *collisions at* $\sqrt{s} = 7$ *TeV*, *Phys. Lett. B* **707** (2012) 52 [arXiv:1109.0963] [INSPIRE].

[39] A. O'Hagan and T. Leonard, *Bayes estimation subject to uncertainty about parameter constraints*, *Biometrika* **63** (1976) 201.

[40] LHCb collaboration, *Observations of* $B_s^0 \to \psi(2S)\eta$ *and* $B_{(s)}^0 \to \psi(2S)\pi^+\pi^-$ *decays*, *Nucl. Phys. B* **871** (2013) 403 [arXiv:1302.6354] [INSPIRE].

[41] E. Govorkova, *Study of* π^0/γ *efficiency using* B *meson decays in the LHCb experiment*, *Phys. Atom. Nucl.* **79** (2016) 1474 [arXiv:1505.02960] [INSPIRE].

[42] LHCb collaboration, *Amplitude analysis of the* $B^+ \to D^+D^-K^+$ *decay*, *Phys. Rev. D* **102** (2020) 112003 [arXiv:2009.00026] [INSPIRE].

[43] A. Poluektov, *Kernel density estimation of a multidimensional efficiency profile*, 2015 *JINST* **10** P02011 [arXiv:1411.5528] [INSPIRE].

[44] LHCb collaboration, *Measurement of relative branching fractions of* B *decays to* ψ(2S) *and* J/ψ *mesons*, *Eur. Phys. J. C* **72** (2012) 2118 [arXiv:1205.0918] [INSPIRE].

[45] LHCb collaboration, *Observation of the* $\Lambda_b^0 \to J/\psi p\pi^-$ *decay*, *JHEP* **07** (2014) 103 [arXiv:1406.0755] [INSPIRE].

[46] N. Cabibbo, *Unitary symmetry and leptonic decays*, *Phys. Rev. Lett.* **10** (1963) 531 [INSPIRE].

JHEP05(2021)095

The LHCb collaboration

R. Aaij[32], C. Abellán Beteta[50], T. Ackernley[60], B. Adeva[46], M. Adinolfi[54], H. Afsharnia[9], C.A. Aidala[85], S. Aiola[25], Z. Ajaltouni[9], S. Akar[65], J. Albrecht[15], F. Alessio[48], M. Alexander[59], A. Alfonso Albero[45], Z. Aliouche[62], G. Alkhazov[38], P. Alvarez Cartelle[55], S. Amato[2], Y. Amhis[11], L. An[48], L. Anderlini[22], A. Andreianov[38], M. Andreotti[21], F. Archilli[17], A. Artamonov[44], M. Artuso[68], K. Arzymatov[42], E. Aslanides[10], M. Atzeni[50], B. Audurier[12], S. Bachmann[17], M. Bachmayer[49], J.J. Back[56], P. Baladron Rodriguez[46], V. Balagura[12], W. Baldini[21], J. Baptista Leite[1], R.J. Barlow[62], S. Barsuk[11], W. Barter[61], M. Bartolini[24], F. Baryshnikov[82], J.M. Basels[14], G. Bassi[29], B. Batsukh[68], A. Battig[15], A. Bay[49], M. Becker[15], F. Bedeschi[29], I. Bediaga[1], A. Beiter[68], V. Belavin[42], S. Belin[27], V. Bellee[49], K. Belous[44], I. Belov[40], I. Belyaev[41], G. Bencivenni[23], E. Ben-Haim[13], A. Berezhnoy[40], R. Bernet[50], D. Berninghoff[17], H.C. Bernstein[68], C. Bertella[48], A. Bertolin[28], C. Betancourt[50], F. Betti[48], Ia. Bezshyiko[50], S. Bhasin[54], J. Bhom[35], L. Bian[73], M.S. Bieker[15], S. Bifani[53], P. Billoir[13], M. Birch[61], F.C.R. Bishop[55], A. Bitadze[62], A. Bizzeti[22,k], M. Bjørn[63], M.P. Blago[48], T. Blake[56], F. Blanc[49], S. Blusk[68], D. Bobulska[59], J.A. Boelhauve[15], O. Boente Garcia[46], T. Boettcher[64], A. Boldyrev[81], A. Bondar[43], N. Bondar[38,48], S. Borghi[62], M. Borisyak[42], M. Borsato[17], J.T. Borsuk[35], S.A. Bouchiba[49], T.J.V. Bowcock[60], A. Boyer[48], C. Bozzi[21], M.J. Bradley[61], S. Braun[66], A. Brea Rodriguez[46], M. Brodski[48], J. Brodzicka[35], A. Brossa Gonzalo[56], D. Brundu[27], A. Buonaura[50], C. Burr[48], A. Bursche[72], A. Butkevich[39], J.S. Butter[32], J. Buytaert[48], W. Byczynski[48], S. Cadeddu[27], H. Cai[73], R. Calabrese[21,f], L. Calefice[15,13], L. Calero Diaz[23], S. Cali[23], R. Calladine[53], M. Calvi[26,j], M. Calvo Gomez[84], P. Camargo Magalhaes[54], A. Camboni[45,84], P. Campana[23], A.F. Campoverde Quezada[6], S. Capelli[26,j], L. Capriotti[20,d], A. Carbone[20,d], G. Carboni[31], R. Cardinale[24], A. Cardini[27], I. Carli[4], P. Carniti[26,j], L. Carus[14], K. Carvalho Akiba[32], A. Casais Vidal[46], G. Casse[60], M. Cattaneo[48], G. Cavallero[48], S. Celani[49], J. Cerasoli[10], A.J. Chadwick[60], M.G. Chapman[54], M. Charles[13], Ph. Charpentier[48], G. Chatzikonstantinidis[53], C.A. Chavez Barajas[60], M. Chefdeville[8], C. Chen[3], S. Chen[4], A. Chernov[35], V. Chobanova[46], S. Cholak[49], M. Chrzaszcz[35], A. Chubykin[38], V. Chulikov[38], P. Ciambrone[23], M.F. Cicala[56], X. Cid Vidal[46], G. Ciezarek[48], P.E.L. Clarke[58], M. Clemencic[48], H.V. Cliff[55], J. Closier[48], J.L. Cobbledick[62], V. Coco[48], J.A.B. Coelho[11], J. Cogan[10], E. Cogneras[9], L. Cojocariu[37], P. Collins[48], T. Colombo[48], L. Congedo[19,c], A. Contu[27], N. Cooke[53], G. Coombs[59], G. Corti[48], C.M. Costa Sobral[56], B. Couturier[48], D.C. Craik[64], J. Crkovská[67], M. Cruz Torres[1], R. Currie[58], C.L. Da Silva[67], E. Dall'Occo[15], J. Dalseno[46], C. D'Ambrosio[48], A. Danilina[41], P. d'Argent[48], A. Davis[62], O. De Aguiar Francisco[62], K. De Bruyn[78], S. De Capua[62], M. De Cian[49], J.M. De Miranda[1], L. De Paula[2], M. De Serio[19,c], D. De Simone[50], P. De Simone[23], J.A. de Vries[79], C.T. Dean[67], D. Decamp[8], L. Del Buono[13], B. Delaney[55], H.-P. Dembinski[15], A. Dendek[34], V. Denysenko[50], D. Derkach[81], O. Deschamps[9], F. Desse[11], F. Dettori[27,e], B. Dey[73], P. Di Nezza[23], S. Didenko[82], L. Dieste Maronas[46], H. Dijkstra[48], V. Dobishuk[52], A.M. Donohoe[18], F. Dordei[27], A.C. dos Reis[1], L. Douglas[59], A. Dovbnya[51], A.G. Downes[8], K. Dreimanis[60], M.W. Dudek[35], L. Dufour[48], V. Duk[77], P. Durante[48], J.M. Durham[67], D. Dutta[62], A. Dziurda[35], A. Dzyuba[38], S. Easo[57], U. Egede[69], V. Egorychev[41], S. Eidelman[43,v], S. Eisenhardt[58], S. Ek-In[49], L. Eklund[59,w], S. Ely[68], A. Ene[37], E. Epple[67], S. Escher[14], J. Eschle[50], S. Esen[13], T. Evans[48], A. Falabella[20], J. Fan[3], Y. Fan[6], B. Fang[73], S. Farry[60], D. Fazzini[26,j], M. Féo[48], A. Fernandez Prieto[46], J.M. Fernandez-tenllado Arribas[45], F. Ferrari[20,d], L. Ferreira Lopes[49], F. Ferreira Rodrigues[2], S. Ferreres Sole[32], M. Ferrillo[50], M. Ferro-Luzzi[48], S. Filippov[39], R.A. Fini[19], M. Fiorini[21,f], M. Firlej[34], K.M. Fischer[63], C. Fitzpatrick[62], T. Fiutowski[34], F. Fleuret[12], M. Fontana[13], F. Fontanelli[24,h], R. Forty[48], V. Franco Lima[60], M. Franco Sevilla[66], M. Frank[48], E. Franzoso[21],

JHEP05(2021)095

G. Frau[17], C. Frei[48], D.A. Friday[59], J. Fu[25], Q. Fuehring[15], W. Funk[48], E. Gabriel[32], T. Gaintseva[42], A. Gallas Torreira[46], D. Galli[20,d], S. Gambetta[58,48], Y. Gan[3], M. Gandelman[2], P. Gandini[25], Y. Gao[5], M. Garau[27], L.M. Garcia Martin[56], P. Garcia Moreno[45], J. García Pardiñas[26], B. Garcia Plana[46], F.A. Garcia Rosales[12], L. Garrido[45], C. Gaspar[48], R.E. Geertsema[32], D. Gerick[17], L.L. Gerken[15], E. Gersabeck[62], M. Gersabeck[62], T. Gershon[56], D. Gerstel[10], Ph. Ghez[8], V. Gibson[55], M. Giovannetti[23,p], A. Gioventù[46], P. Gironella Gironell[45], L. Giubega[37], C. Giugliano[21,f,48], K. Gizdov[58], E.L. Gkougkousis[48], V.V. Gligorov[13], C. Göbel[70], E. Golobardes[84], D. Golubkov[41], A. Golutvin[61,82], A. Gomes[1,a], S. Gomez Fernandez[45], F. Goncalves Abrantes[63], M. Goncerz[35], G. Gong[3], P. Gorbounov[41], I.V. Gorelov[40], C. Gotti[26], E. Govorkova[48], J.P. Grabowski[17], T. Grammatico[13], L.A. Granado Cardoso[48], E. Graugés[45], E. Graverini[49], G. Graziani[22], A. Grecu[37], L.M. Greeven[32], P. Griffith[21,f], L. Grillo[62], S. Gromov[82], B.R. Gruberg Cazon[63], C. Gu[3], M. Guarise[21], P. A. Günther[17], E. Gushchin[39], A. Guth[14], Y. Guz[44,48], T. Gys[48], T. Hadavizadeh[69], G. Haefeli[49], C. Haen[48], J. Haimberger[48], T. Halewood-leagas[60], P.M. Hamilton[66], Q. Han[7], X. Han[17], T.H. Hancock[63], S. Hansmann-Menzemer[17], N. Harnew[63], T. Harrison[60], C. Hasse[48], M. Hatch[48], J. He[6,b], M. Hecker[61], K. Heijhoff[32], K. Heinicke[15], A.M. Hennequin[48], K. Hennessy[60], L. Henry[25,47], J. Heuel[14], A. Hicheur[2], D. Hill[49], M. Hilton[62], S.E. Hollitt[15], J. Hu[17], J. Hu[72], W. Hu[7], W. Huang[6], X. Huang[73], W. Hulsbergen[32], R.J. Hunter[56], M. Hushchyn[81], D. Hutchcroft[60], D. Hynds[32], P. Ibis[15], M. Idzik[34], D. Ilin[38], P. Ilten[65], A. Inglessi[38], A. Ishteev[82], K. Ivshin[38], R. Jacobsson[48], S. Jakobsen[48], E. Jans[32], B.K. Jashal[47], A. Jawahery[66], V. Jevtic[15], M. Jezabek[35], F. Jiang[3], M. John[63], D. Johnson[48], C.R. Jones[55], T.P. Jones[56], B. Jost[48], N. Jurik[48], S. Kandybei[51], Y. Kang[3], M. Karacson[48], M. Karpov[81], F. Keizer[55,48], M. Kenzie[56], T. Ketel[33], B. Khanji[15], A. Kharisova[83], S. Kholodenko[44], T. Kirn[14], V.S. Kirsebom[49], O. Kitouni[64], S. Klaver[32], K. Klimaszewski[36], S. Koliiev[52], A. Kondybayeva[82], A. Konoplyannikov[41], P. Kopciewicz[34], R. Kopecna[17], P. Koppenburg[32], M. Korolev[40], I. Kostiuk[32,52], O. Kot[52], S. Kotriakhova[f,38], P. Kravchenko[38], L. Kravchuk[39], R.D. Krawczyk[48], M. Kreps[56], F. Kress[61], S. Kretzschmar[14], P. Krokovny[43,v], W. Krupa[34], W. Krzemien[36], W. Kucewicz[35,t], M. Kucharczyk[35], V. Kudryavtsev[43,v], H.S. Kuindersma[32], G.J. Kunde[67], T. Kvaratskheliya[41], D. Lacarrere[48], G. Lafferty[62], A. Lai[27], A. Lampis[27], D. Lancierini[50], J.J. Lane[62], R. Lane[54], G. Lanfranchi[23], C. Langenbruch[14], J. Langer[15], O. Lantwin[50], T. Latham[56], F. Lazzari[29,q], R. Le Gac[10], S.H. Lee[85], R. Lefèvre[9], A. Leflat[40], S. Legotin[82], O. Leroy[10], T. Lesiak[35], B. Leverington[17], H. Li[72], L. Li[63], P. Li[17], S. Li[7], Y. Li[4], Y. Li[4], Z. Li[68], X. Liang[68], T. Lin[61], R. Lindner[48], V. Lisovskyi[15], R. Litvinov[27], G. Liu[72], H. Liu[6], S. Liu[4], X. Liu[3], A. Loi[27], J. Lomba Castro[46], I. Longstaff[59], J.H. Lopes[2], G.H. Lovell[55], Y. Lu[4], D. Lucchesi[28,l], S. Luchuk[39], M. Lucio Martinez[32], V. Lukashenko[32], Y. Luo[3], A. Lupato[62], E. Luppi[21,f], O. Lupton[56], A. Lusiani[29,m], X. Lyu[6], L. Ma[4], R. Ma[6], S. Maccolini[20,d], F. Machefert[11], F. Maciuc[37], V. Macko[49], P. Mackowiak[15], S. Maddrell-Mander[54], O. Madejczyk[34], L.R. Madhan Mohan[54], O. Maev[38], A. Maevskiy[81], D. Maisuzenko[38], M.W. Majewski[34], J.J. Malczewski[35], S. Malde[63], B. Malecki[48], A. Malinin[80], T. Maltsev[43,v], H. Malygina[17], G. Manca[27,e], G. Mancinelli[10], D. Manuzzi[20,d], D. Marangotto[25,i], J. Maratas[9,s], J.F. Marchand[8], U. Marconi[20], S. Mariani[22,g], C. Marin Benito[11], M. Marinangeli[49], P. Marino[49,m], J. Marks[17], A.M. Marshall[54], P.J. Marshall[60], G. Martellotti[30], L. Martinazzoli[48,j], M. Martinelli[26,j], D. Martinez Santos[46], F. Martinez Vidal[47], A. Massafferri[1], M. Materok[14], R. Matev[48], A. Mathad[50], Z. Mathe[48], V. Matiunin[41], C. Matteuzzi[26], K.R. Mattioli[85], A. Mauri[32], E. Maurice[12], J. Mauricio[45], M. Mazurek[36], M. McCann[61], L. Mcconnell[18], T.H. Mcgrath[62], A. McNab[62], R. McNulty[18], J.V. Mead[60], B. Meadows[65], C. Meaux[10], G. Meier[15], N. Meinert[76], D. Melnychuk[36], S. Meloni[26,j], M. Merk[32,79], A. Merli[25], L. Meyer Garcia[2], M. Mikhasenko[48], D.A. Milanes[74], E. Millard[56], M. Milovanovic[48],

JHEP05(2021)095

M.-N. Minard[8], A. Minotti[21], L. Minzoni[21,f], S.E. Mitchell[58], B. Mitreska[62], D.S. Mitzel[48], A. Mödden [15], R.A. Mohammed[63], R.D. Moise[61], T. Mombächer[15], I.A. Monroy[74], S. Monteil[9], M. Morandin[28], G. Morello[23], M.J. Morello[29,m], J. Moron[34], A.B. Morris[75], A.G. Morris[56], R. Mountain[68], H. Mu[3], F. Muheim[58,48], M. Mukherjee[7], M. Mulder[48], D. Müller[48], K. Müller[50], C.H. Murphy[63], D. Murray[62], P. Muzzetto[27,48], P. Naik[54], T. Nakada[49], R. Nandakumar[57], T. Nanut[49], I. Nasteva[2], M. Needham[58], I. Neri[21], N. Neri[25,i], S. Neubert[75], N. Neufeld[48], R. Newcombe[61], T.D. Nguyen[49], C. Nguyen-Mau[49,x], E.M. Niel[11], S. Nieswand[14], N. Nikitin[40], N.S. Nolte[48], C. Nunez[85], A. Oblakowska-Mucha[34], V. Obraztsov[44], D.P. O'Hanlon[54], R. Oldeman[27,e], M.E. Olivares[68], C.J.G. Onderwater[78], A. Ossowska[35], J.M. Otalora Goicochea[2], T. Ovsiannikova[41], P. Owen[50], A. Oyanguren[47], B. Pagare[56], P.R. Pais[48], T. Pajero[63], A. Palano[19], M. Palutan[23], Y. Pan[62], G. Panshin[83], A. Papanestis[57], M. Pappagallo[19,c], L.L. Pappalardo[21,f], C. Pappenheimer[65], W. Parker[66], C. Parkes[62], C.J. Parkinson[46], B. Passalacqua[21], G. Passaleva[22], A. Pastore[19], M. Patel[61], C. Patrignani[20,d], C.J. Pawley[79], A. Pearce[48], A. Pellegrino[32], M. Pepe Altarelli[48], S. Perazzini[20], D. Pereima[41], P. Perret[9], M. Petric[59,48], K. Petridis[54], A. Petrolini[24,h], A. Petrov[80], S. Petrucci[58], M. Petruzzo[25], T.T.H. Pham[68], A. Philippov[42], L. Pica[29,n], M. Piccini[77], B. Pietrzyk[8], G. Pietrzyk[49], M. Pili[63], D. Pinci[30], F. Pisani[48], Resmi P.K[10], V. Placinta[37], J. Plews[53], M. Plo Casasus[46], F. Polci[13], M. Poli Lener[23], M. Poliakova[68], A. Poluektov[10], N. Polukhina[82,u], I. Polyakov[68], E. Polycarpo[2], G.J. Pomery[54], S. Ponce[48], D. Popov[6,48], S. Popov[42], S. Poslavskii[44], K. Prasanth[35], L. Promberger[48], C. Prouve[46], V. Pugatch[52], H. Pullen[63], G. Punzi[29,n], W. Qian[6], J. Qin[6], R. Quagliani[13], B. Quintana[8], N.V. Raab[18], R.I. Rabadan Trejo[10], B. Rachwal[34], J.H. Rademacker[54], M. Rama[29], M. Ramos Pernas[56], M.S. Rangel[2], F. Ratnikov[42,81], G. Raven[33], M. Reboud[8], F. Redi[49], F. Reiss[62], C. Remon Alepuz[47], Z. Ren[3], V. Renaudin[63], R. Ribatti[29], S. Ricciardi[57], K. Rinnert[60], P. Robbe[11], A. Robert[13], G. Robertson[58], A.B. Rodrigues[49], E. Rodrigues[60], J.A. Rodriguez Lopez[74], A. Rollings[63], P. Roloff[48], V. Romanovskiy[44], M. Romero Lamas[46], A. Romero Vidal[46], J.D. Roth[85], M. Rotondo[23], M.S. Rudolph[68], T. Ruf[48], J. Ruiz Vidal[47], A. Ryzhikov[81], J. Ryzka[34], J.J. Saborido Silva[46], N. Sagidova[38], N. Sahoo[56], B. Saitta[27,e], D. Sanchez Gonzalo[45], C. Sanchez Gras[32], R. Santacesaria[30], C. Santamarina Rios[46], M. Santimaria[23], E. Santovetti[31,p], D. Saranin[82], G. Sarpis[59], M. Sarpis[75], A. Sarti[30], C. Satriano[30,o], A. Satta[31], M. Saur[15], D. Savrina[41,40], H. Sazak[9], L.G. Scantlebury Smead[63], S. Schael[14], M. Schellenberg[15], M. Schiller[59], H. Schindler[48], M. Schmelling[16], B. Schmidt[48], O. Schneider[49], A. Schopper[48], M. Schubiger[32], S. Schulte[49], M.H. Schune[11], R. Schwemmer[48], B. Sciascia[23], S. Sellam[46], A. Semennikov[41], M. Senghi Soares[33], A. Sergi[24,48], N. Serra[50], L. Sestini[28], A. Seuthe[15], P. Seyfert[48], Y. Shang[5], D.M. Shangase[85], M. Shapkin[44], I. Shchemerov[82], L. Shchutska[49], T. Shears[60], L. Shekhtman[43,v], Z. Shen[5], V. Shevchenko[80], E.B. Shields[26,j], E. Shmanin[82], J.D. Shupperd[68], B.G. Siddi[21], R. Silva Coutinho[50], G. Simi[28], S. Simone[19,c], N. Skidmore[62], T. Skwarnicki[68], M.W. Slater[53], I. Slazyk[21,f], J.C. Smallwood[63], J.G. Smeaton[55], A. Smetkina[41], E. Smith[14], M. Smith[61], A. Snoch[32], M. Soares[20], L. Soares Lavra[9], M.D. Sokoloff[65], F.J.P. Soler[59], A. Solovev[38], I. Solovyev[38], F.L. Souza De Almeida[2], B. Souza De Paula[2], B. Spaan[15], E. Spadaro Norella[25,i], P. Spradlin[59], F. Stagni[48], M. Stahl[65], S. Stahl[48], P. Stefko[49], O. Steinkamp[50,82], O. Stenyakin[44], H. Stevens[15], S. Stone[68], M.E. Stramaglia[49], M. Straticiuc[37], D. Strekalina[82], F. Suljik[63], J. Sun[27], L. Sun[73], Y. Sun[66], P. Svihra[62], P.N. Swallow[53], K. Swientek[34], A. Szabelski[36], T. Szumlak[34], M. Szymanski[48], S. Taneja[62], F. Teubert[48], E. Thomas[48], K.A. Thomson[60], V. Tisserand[9], S. T'Jampens[8], M. Tobin[4], L. Tomassetti[21,f], D. Torres Machado[1], D.Y. Tou[13], M.T. Tran[49], E. Trifonova[82], C. Trippl[49], G. Tuci[29,n], A. Tully[49], N. Tuning[32,48], A. Ukleja[36], D.J. Unverzagt[17], E. Ursov[82], A. Usachov[32], A. Ustyuzhanin[42,81], U. Uwer[17], A. Vagner[83], V. Vagnoni[20], A. Valassi[48], G. Valenti[20], N. Valls Canudas[45], M. van Beuzekom[32], M. Van Dijk[49],

JHEP05(2021)095

E. van Herwijnen[82], C.B. Van Hulse[18], M. van Veghel[78], R. Vazquez Gomez[46], P. Vazquez Regueiro[46], C. Vázquez Sierra[48], S. Vecchi[21], J.J. Velthuis[54], M. Veltri[22,r], A. Venkateswaran[68], M. Veronesi[32], M. Vesterinen[56], D. Vieira[65], M. Vieites Diaz[49], H. Viemann[76], X. Vilasis-Cardona[84], E. Vilella Figueras[60], P. Vincent[13], G. Vitali[29], D. Vom Bruch[10], A. Vorobyev[38], V. Vorobyev[43,v], N. Voropaev[38], R. Waldi[76], J. Walsh[29], C. Wang[17], J. Wang[5], J. Wang[4], J. Wang[3], J. Wang[73], M. Wang[3], R. Wang[54], Y. Wang[7], Z. Wang[50], Z. Wang[3], H.M. Wark[60], N.K. Watson[53], S.G. Weber[13], D. Websdale[61], C. Weisser[64], B.D.C. Westhenry[54], D.J. White[62], M. Whitehead[54], D. Wiedner[15], G. Wilkinson[63], M. Wilkinson[68], I. Williams[55], M. Williams[64], M.R.J. Williams[58], F.F. Wilson[57], W. Wislicki[36], M. Witek[35], L. Witola[17], G. Wormser[11], S.A. Wotton[55], H. Wu[68], K. Wyllie[48], Z. Xiang[6], D. Xiao[7], Y. Xie[7], A. Xu[5], J. Xu[6], L. Xu[3], M. Xu[7], Q. Xu[6], Z. Xu[5], Z. Xu[6], D. Yang[3], S. Yang[6], Y. Yang[6], Z. Yang[3], Z. Yang[66], Y. Yao[68], L.E. Yeomans[60], H. Yin[7], J. Yu[71], X. Yuan[68], O. Yushchenko[44], E. Zaffaroni[49], M. Zavertyaev[16,u], M. Zdybal[35], O. Zenaiev[48], M. Zeng[3], D. Zhang[7], L. Zhang[3], S. Zhang[5], Y. Zhang[5], Y. Zhang[63], A. Zhelezov[17], Y. Zheng[6], X. Zhou[6], Y. Zhou[6], X. Zhu[3], V. Zhukov[14,40], J.B. Zonneveld[58], Q. Zou[4], S. Zucchelli[20,d], D. Zuliani[28], G. Zunica[62]

[1] *Centro Brasileiro de Pesquisas Físicas (CBPF), Rio de Janeiro, Brazil*
[2] *Universidade Federal do Rio de Janeiro (UFRJ), Rio de Janeiro, Brazil*
[3] *Center for High Energy Physics, Tsinghua University, Beijing, China*
[4] *Institute Of High Energy Physics (IHEP), Beijing, China*
[5] *School of Physics State Key Laboratory of Nuclear Physics and Technology, Peking University, Beijing, China*
[6] *University of Chinese Academy of Sciences, Beijing, China*
[7] *Institute of Particle Physics, Central China Normal University, Wuhan, Hubei, China*
[8] *Univ. Grenoble Alpes, Univ. Savoie Mont Blanc, CNRS, IN2P3-LAPP, Annecy, France*
[9] *Université Clermont Auvergne, CNRS/IN2P3, LPC, Clermont-Ferrand, France*
[10] *Aix Marseille Univ, CNRS/IN2P3, CPPM, Marseille, France*
[11] *Université Paris-Saclay, CNRS/IN2P3, IJCLab, Orsay, France*
[12] *Laboratoire Leprince-Ringuet, CNRS/IN2P3, Ecole Polytechnique, Institut Polytechnique de Paris, Palaiseau, France*
[13] *LPNHE, Sorbonne Université, Paris Diderot Sorbonne Paris Cité, CNRS/IN2P3, Paris, France*
[14] *I. Physikalisches Institut, RWTH Aachen University, Aachen, Germany*
[15] *Fakultät Physik, Technische Universität Dortmund, Dortmund, Germany*
[16] *Max-Planck-Institut für Kernphysik (MPIK), Heidelberg, Germany*
[17] *Physikalisches Institut, Ruprecht-Karls-Universität Heidelberg, Heidelberg, Germany*
[18] *School of Physics, University College Dublin, Dublin, Ireland*
[19] *INFN Sezione di Bari, Bari, Italy*
[20] *INFN Sezione di Bologna, Bologna, Italy*
[21] *INFN Sezione di Ferrara, Ferrara, Italy*
[22] *INFN Sezione di Firenze, Firenze, Italy*
[23] *INFN Laboratori Nazionali di Frascati, Frascati, Italy*
[24] *INFN Sezione di Genova, Genova, Italy*
[25] *INFN Sezione di Milano, Milano, Italy*
[26] *INFN Sezione di Milano-Bicocca, Milano, Italy*
[27] *INFN Sezione di Cagliari, Monserrato, Italy*
[28] *Universita degli Studi di Padova, Universita e INFN, Padova, Padova, Italy*
[29] *INFN Sezione di Pisa, Pisa, Italy*
[30] *INFN Sezione di Roma La Sapienza, Roma, Italy*
[31] *INFN Sezione di Roma Tor Vergata, Roma, Italy*
[32] *Nikhef National Institute for Subatomic Physics, Amsterdam, Netherlands*

JHEP05(2021)095

[33] Nikhef National Institute for Subatomic Physics and VU University Amsterdam, Amsterdam, Netherlands
[34] AGH - University of Science and Technology, Faculty of Physics and Applied Computer Science, Kraków, Poland
[35] Henryk Niewodniczanski Institute of Nuclear Physics Polish Academy of Sciences, Kraków, Poland
[36] National Center for Nuclear Research (NCBJ), Warsaw, Poland
[37] Horia Hulubei National Institute of Physics and Nuclear Engineering, Bucharest-Magurele, Romania
[38] Petersburg Nuclear Physics Institute NRC Kurchatov Institute (PNPI NRC KI), Gatchina, Russia
[39] Institute for Nuclear Research of the Russian Academy of Sciences (INR RAS), Moscow, Russia
[40] Institute of Nuclear Physics, Moscow State University (SINP MSU), Moscow, Russia
[41] Institute of Theoretical and Experimental Physics NRC Kurchatov Institute (ITEP NRC KI), Moscow, Russia
[42] Yandex School of Data Analysis, Moscow, Russia
[43] Budker Institute of Nuclear Physics (SB RAS), Novosibirsk, Russia
[44] Institute for High Energy Physics NRC Kurchatov Institute (IHEP NRC KI), Protvino, Russia, Protvino, Russia
[45] ICCUB, Universitat de Barcelona, Barcelona, Spain
[46] Instituto Galego de Física de Altas Enerxías (IGFAE), Universidade de Santiago de Compostela, Santiago de Compostela, Spain
[47] Instituto de Fisica Corpuscular, Centro Mixto Universidad de Valencia - CSIC, Valencia, Spain
[48] European Organization for Nuclear Research (CERN), Geneva, Switzerland
[49] Institute of Physics, Ecole Polytechnique Fédérale de Lausanne (EPFL), Lausanne, Switzerland
[50] Physik-Institut, Universität Zürich, Zürich, Switzerland
[51] NSC Kharkiv Institute of Physics and Technology (NSC KIPT), Kharkiv, Ukraine
[52] Institute for Nuclear Research of the National Academy of Sciences (KINR), Kyiv, Ukraine
[53] University of Birmingham, Birmingham, United Kingdom
[54] H.H. Wills Physics Laboratory, University of Bristol, Bristol, United Kingdom
[55] Cavendish Laboratory, University of Cambridge, Cambridge, United Kingdom
[56] Department of Physics, University of Warwick, Coventry, United Kingdom
[57] STFC Rutherford Appleton Laboratory, Didcot, United Kingdom
[58] School of Physics and Astronomy, University of Edinburgh, Edinburgh, United Kingdom
[59] School of Physics and Astronomy, University of Glasgow, Glasgow, United Kingdom
[60] Oliver Lodge Laboratory, University of Liverpool, Liverpool, United Kingdom
[61] Imperial College London, London, United Kingdom
[62] Department of Physics and Astronomy, University of Manchester, Manchester, United Kingdom
[63] Department of Physics, University of Oxford, Oxford, United Kingdom
[64] Massachusetts Institute of Technology, Cambridge, MA, United States
[65] University of Cincinnati, Cincinnati, OH, United States
[66] University of Maryland, College Park, MD, United States
[67] Los Alamos National Laboratory (LANL), Los Alamos, United States
[68] Syracuse University, Syracuse, NY, United States
[69] School of Physics and Astronomy, Monash University, Melbourne, Australia, associated to [56]
[70] Pontifícia Universidade Católica do Rio de Janeiro (PUC-Rio), Rio de Janeiro, Brazil, associated to [2]
[71] Physics and Micro Electronic College, Hunan University, Changsha City, China, associated to [7]
[72] Guangdong Provencial Key Laboratory of Nuclear Science, Institute of Quantum Matter, South China Normal University, Guangzhou, China, associated to [3]
[73] School of Physics and Technology, Wuhan University, Wuhan, China, associated to [3]
[74] Departamento de Fisica, Universidad Nacional de Colombia, Bogota, Colombia, associated to [13]
[75] Universität Bonn - Helmholtz-Institut für Strahlen und Kernphysik, Bonn, Germany, associated to [17]

JHEP05(2021)095

[76] *Institut für Physik, Universität Rostock, Rostock, Germany, associated to* [17]
[77] *INFN Sezione di Perugia, Perugia, Italy, associated to* [21]
[78] *Van Swinderen Institute, University of Groningen, Groningen, Netherlands, associated to* [32]
[79] *Universiteit Maastricht, Maastricht, Netherlands, associated to* [32]
[80] *National Research Centre Kurchatov Institute, Moscow, Russia, associated to* [41]
[81] *National Research University Higher School of Economics, Moscow, Russia, associated to* [42]
[82] *National University of Science and Technology "MISIS", Moscow, Russia, associated to* [41]
[83] *National Research Tomsk Polytechnic University, Tomsk, Russia, associated to* [41]
[84] *DS4DS, La Salle, Universitat Ramon Llull, Barcelona, Spain, associated to* [45]
[85] *University of Michigan, Ann Arbor, United States, associated to* [68]

[a] *Universidade Federal do Triângulo Mineiro (UFTM), Uberaba-MG, Brazil*
[b] *Hangzhou Institute for Advanced Study, UCAS, Hangzhou, China*
[c] *Università di Bari, Bari, Italy*
[d] *Università di Bologna, Bologna, Italy*
[e] *Università di Cagliari, Cagliari, Italy*
[f] *Università di Ferrara, Ferrara, Italy*
[g] *Università di Firenze, Firenze, Italy*
[h] *Università di Genova, Genova, Italy*
[i] *Università degli Studi di Milano, Milano, Italy*
[j] *Università di Milano Bicocca, Milano, Italy*
[k] *Università di Modena e Reggio Emilia, Modena, Italy*
[l] *Università di Padova, Padova, Italy*
[m] *Scuola Normale Superiore, Pisa, Italy*
[n] *Università di Pisa, Pisa, Italy*
[o] *Università della Basilicata, Potenza, Italy*
[p] *Università di Roma Tor Vergata, Roma, Italy*
[q] *Università di Siena, Siena, Italy*
[r] *Università di Urbino, Urbino, Italy*
[s] *MSU - Iligan Institute of Technology (MSU-IIT), Iligan, Philippines*
[t] *AGH - University of Science and Technology, Faculty of Computer Science, Electronics and Telecommunications, Kraków, Poland*
[u] *P.N. Lebedev Physical Institute, Russian Academy of Science (LPI RAS), Moscow, Russia*
[v] *Novosibirsk State University, Novosibirsk, Russia*
[w] *Department of Physics and Astronomy, Uppsala University, Uppsala, Sweden*
[x] *Hanoi University of Science, Hanoi, Vietnam*

JHEP05(2021)095